

# Influence of hydrometeors on InSAR observations

Dmitri Moisseev and Ramon Hanssen  
 Faculty of Civil Engineering and Geosciences  
 Thijsseweg 11, 2629JA Delft, The Netherlands  
 e-mail: d.moisseev@citg.tudelft.nl

**Abstract**—Repeat-pass synthetic aperture radar interferometry is an important tool for measuring earth surface topography and/or surface deformations. These observations, however, are highly affected by the atmosphere. Therefore, an accurate description of atmospheric distortions is very important to improve an accuracy of interferometric measurements. In this paper we discuss influence of hydrometeors on the microwave propagation. On examples of two interferograms we show that there is a strong increase in a propagation delay associated with rain. To validate this observation we have used weather radar measurements to estimate contribution of rain droplets on the propagation path. It is shown that in some cases, a rain induced propagation delay can be of several centimeters.

**Keywords**—SAR interferometry; radiowave propagation; precipitation

## I. SAR INTERFEROMETRY AND ATMOSPHERIC PHASE DELAY

The ERS-1,2 and ENVISAT SAR measurements provide a high resolution measurements of the earth surface. A phase value of every resolution cell is defined as a superposition of the term which corresponds to the geometric distance,  $\Psi_{\text{geo}}$ , a term which corresponds to propagation effects,  $\Psi_{\text{prop}}$ , and the term which represents the scattering within the resolution cell,  $\Psi_{\text{scat}}$ . By creating an interferogram, effectively the phases corresponding to two measurements are subtracted from each other

$$\Delta\Psi = \Delta\Psi_{\text{geo}} + \Delta\Psi_{\text{prop}} + \Delta\Psi_{\text{scat}} \quad (1)$$

and if objects within resolution cells did not move and did not change from one acquisition to the other, the differential phase is mainly defined by the propagation effects and the difference in observation geometries. Furthermore, if a reference elevation model is available one can remove the topographic phase component. The remaining phase would fully be determined by the propagation through the ionosphere,  $\Delta\Psi_{\text{iono}}$ , and atmosphere,  $\Delta\Psi_{\text{atm}}$ :

$$\begin{aligned} \Delta\Psi_{\text{prop}} &= \Delta\Psi_{\text{iono}} + \Delta\Psi_{\text{atm}} \\ &= \Delta\Psi_{\text{iono}} + (\Delta\Psi_{\text{hydr}} + \Delta\Psi_{\text{wet}} + \Delta\Psi_{\text{liquid}}) \end{aligned} \quad (2)$$

the atmospheric component in its turn depends on hydrostatic part, propagation through the dry atmosphere, wet delay, propagation through water vapor and liquid part, caused by propagation through volume filled with liquid droplets.

The hydrostatic and ionospheric parts have the largest contribution to the total phase delay. A variability of these

delays, however, have mainly a rather long wavelength as compared to the spatial extend of an interferogram and thus their contribution can easily be suppressed. The wet and liquid delays, on the other hand, contribute less to the total delay, but spatial behavior of these delays is more stochastic and therefore it is more difficult to compensate for them. In this article we will discuss influence of precipitation on the atmospheric phase delay. Moreover, we will illustrate our study by two comparisons of weather radar rain rate measurements to atmospheric phase delay observations as acquired by ERS-1,2 during the tandem mission in 1995-96.

## II. HYDROMETEORS CONTRIBUTION TO ATMOSPHERIC PHASE DELAY

### A. Signal delay induced by scattering in rain

It was shown in [3, 5] that for the case of coherent propagation in rain the propagation phase delay,  $\delta$  in mm/km, can be calculated as

$$\delta = 10^{-3} \frac{2\pi}{k^2} \int \text{Re}(f(D)N(D))dD \quad (3)$$

where  $k$  is the wave number (wavelength is 56 mm),  $D$  is the equivolumic drop diameter,  $f(D)$  is the forward scattering amplitude in millimeters and  $N(D)$  is the drop size distribution given in  $\text{mm}^{-1}\text{m}^{-3}$ .

Commonly the drop size distribution is assumed to have an exponential form [4]

$$N(D) = N_0 \exp(-AD) \quad (4)$$

where  $N_0 = 8000 \text{ mm}^{-1}\text{m}^{-3}$  and

$$A = 4.1/R^{0.21} \quad (5)$$

where  $R$  is the rain rate given in mm/hr.

To estimate the scattering amplitude it is common to model the raindrops that are larger than 1 mm as oblate spheroids with the ratio of the horizontal to vertical axis  $e$  related to the equivolumic drop diameter  $D$  as [6]

$$e = 1.03 - 0.062 D \quad (6)$$

In this case using Rayleigh approximation [5] the scattered amplitude for  $h$ -polarized incidence wave can be calculated as:

$$f(D) = \frac{k^2}{24} D^3 (\varepsilon - 1) A \quad (7)$$

where  $\epsilon$  is the relative permittivity of water and  $\Lambda$  is

$$\Lambda = \frac{1}{1 + \lambda(\epsilon - 1)}$$

where

$$\lambda = \frac{1 - \lambda_3}{2}, \text{ and } \lambda_3 = \frac{1 + f^2}{f^2} \left(1 - \frac{1}{f} \tan^{-1} f\right)$$

$$\text{where } f = e^{-2} - 1 \quad (8)$$

Using equations (3)-(8) we can calculate the path delay for different rain intensities. It should be noted that raindrop diameter is usually truncated at 8 mm, since particles with a larger diameter are unstable.

In Figure 1 the result of these calculations is given. It can be seen that for high rain intensities the path delay can be as high as several centimeters.

### III. OBSERVATIONS

#### A. InSAR observations

For this study we have used two interferograms. Both interferograms were acquired over Flevoland in the Netherlands. This area in the Netherlands is known for its extremely flat landscape. Since both interferograms were acquired with only one day difference in the satellites overpasses, no earth surface deformations are expected.

The first interferogram was acquired at October 3 and 4, 1995 at 21.41 UTC. SAR frame numbers are 1053 and 1035, for ERS-1 orbit 22061 and ERS-2 orbit 2388, see Figure 2. The perpendicular baseline 385 and 393 m. This interferogram is a composition of two neighboring scenes.

The second interferogram was acquired at August 29 and 30, 1995, at 21.41 UTC. SAR frame number 1035, for ERS-1 orbit 21560 and ERS-2 orbit 1887. The perpendicular baseline is 80 m. The interferogram is shown in Figure 3.

For these interferograms a phase unwrapping is performed using the minimal cost flow algorithm [7]. After the unwrapping the reference digital elevation model (DEM) was used to remove the topography. Furthermore, the spatial resolution was reduced to 160 x 160 m to reduce the speckle.

To eliminate the hydrostatic component of the atmosphere Saastamoinen model [8] of neutral atmosphere is used. This model allows for hydrostatic delay estimates with an accuracy of 1 mm or better [9]. Moreover, the mean delay value calculated over the complete interferogram was calculated and subtracted for each interferogram. This processing step allows reducing an effect of ionosphere on the delay measurements, since an ionospheric delay has only long wavelength variability. Therefore, the remaining delay signal after all the processing steps is expected to be only due to propagation through the moist air and scattering on hydrometeors.

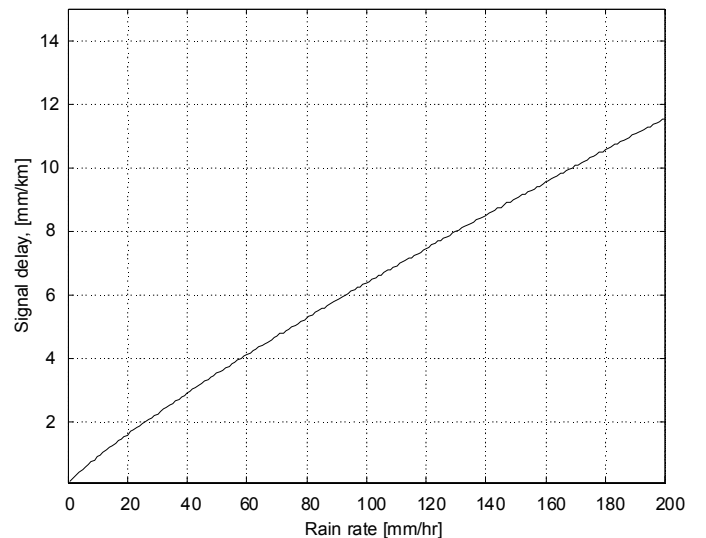


Figure 1. Path delay as a function of the rain rate. This calculations are done for HH polarization of the transmit and receive antenna.

#### B. Weather radar data

The weather radar data are the combination of two weather radars located in Schiphol and De Bilt, the Netherlands. These two radars are operating in C-band. Measurements from these two radars are combined into the reflectivity mosaic that covers completely the Netherlands. This mosaic is available every 15 min. From the observed reflectivity the rain rate is calculated using a standard Z-R relation

$$Z = 200R^{1.6} \quad (9)$$

It should be noted that this relationship accuracy can be a factor 3 too large or too small [2] and that causes one the main uncertainties in the phase delay calculations.

### IV. DISCUSSION

In Figures 2 and 3 comparisons between weather radar and InSAR measurements are shown. It can be seen that in all the cases the propagation delays caused by raindrops are much smaller than the observed delay. To estimate the signal delays due to the rain, we have use equation (1) –(8) to calculate path delay per km. Then, from radiosonde data we have obtained the height of zero isotherm which was used to estimate the total path through the rain.

It should be noted that these calculations do not include estimations of the delay due to the melting layer of precipitations and due to the precipitating cloud above the melting layer. However, we expect that contribution of the melting layer is rather limited since it occupies the limited height range (usually in the order of few hundred meters). The precipitating cloud on the other hand can have a rather large height range, but due to the fact that the relative permittivity of ice is much smaller than the one of water the contribution of the precipitating cloud to the signal delay would be negligible.

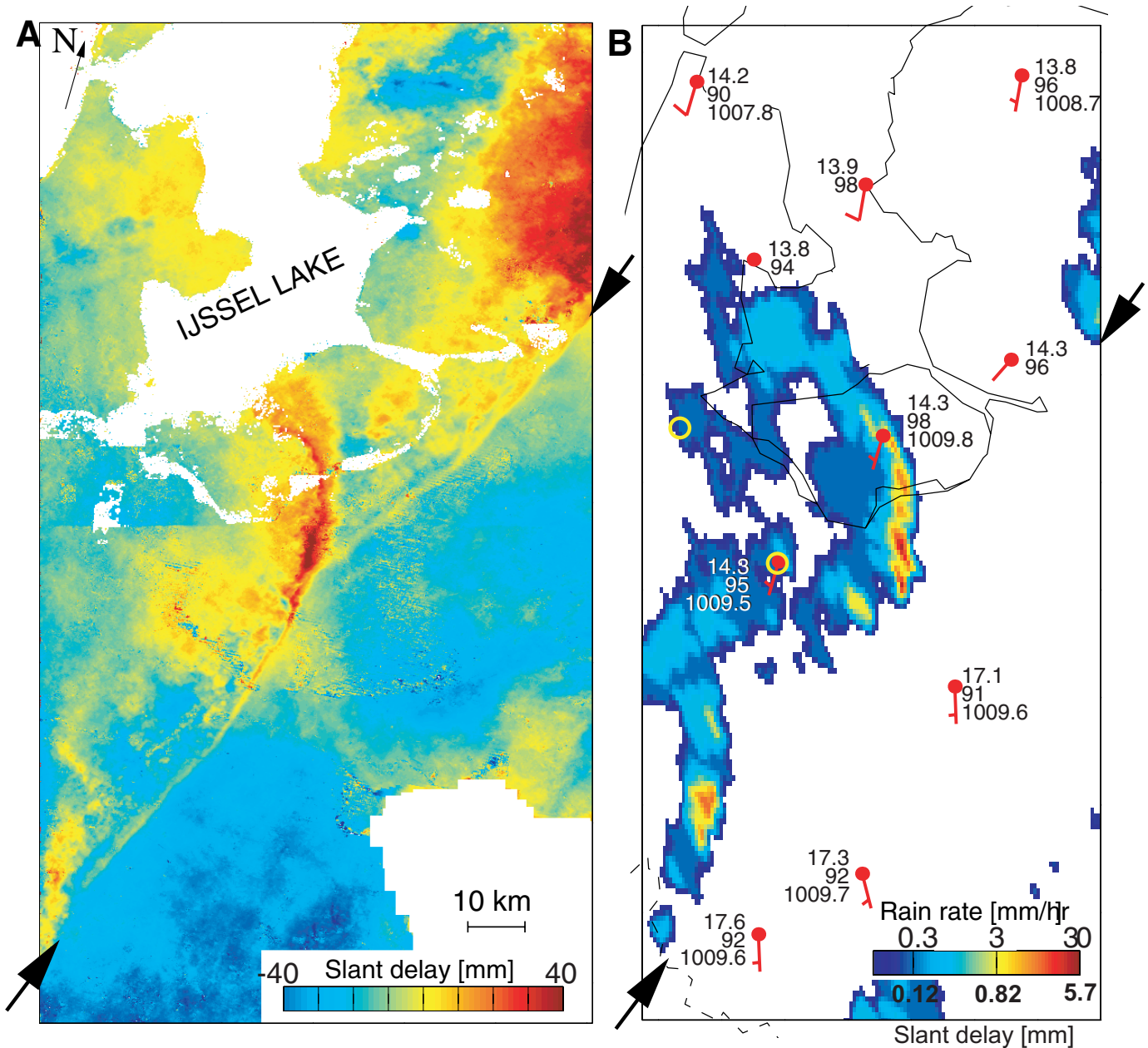


Figure 2. The cold front observation. (A) SAR interferogram of 3 and 4 October 1995, 21.41 UTC. The boundary of the cold front is clearly visible. (B) Weather radar image from 4 October 1995, 21.45 UTC. It can be seen that areas of large slant delay correspond to the areas of high rain intensity. In Figure 2 (B) the rain rate is recalculated to the slant delay. It can be observed that propagation through rain alone cannot explain high values of the observed slant delay.

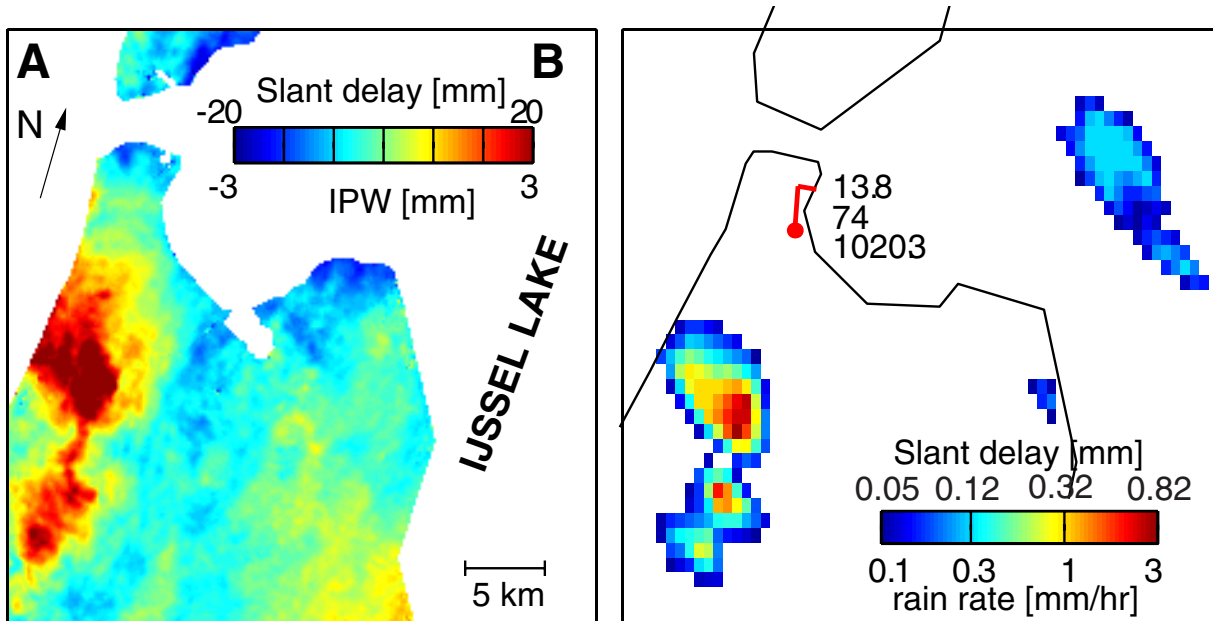


Figure 3. Precipitation measurement. (A) SAR interferogram acquired on 29 and 30 August 1995. (B) Weather radar measurement taken on 29 August 1995. In this figure both rain rate and slant delay are depicted. It can also be seen that slant delay caused by propagation through the precipitation media is much smaller than the observed one.

It was discussed in [1] that neither changes in pressure nor changes in temperature can explain the enhanced slant delay in the rain area. Therefore, the most probable explanation would be an increase in the water vapor concentration due to partial evaporation of the raindrops.

## V. CONCLUSIONS

In this paper influence of rain on InSAR measurements was studied. It was shown that for a hard rain the signal delay caused by rain can be as large as several centimeters. This effect would mainly be observed in tropical climate. Based on two examples it was shown that precipitation does cause an enhanced signal delay, but the most probable explanation of this effect is an increase in water vapor concentration due to partial evaporation of raindrops.

## ACKNOWLEDGMENT

The authors would like to thank Dr. Nikolaos Skaropoulos for the valuable comments on the scattering calculations. The authors would also like to thank the ESA for providing the ERS-1, 2 SAR measurements and the KNMI for providing the weather radar data.

## REFERENCES

- [1] R. Hanssen, Radar Interferometry. Data interpretation and error analysis. Dordrecht, Kluwer Academic Publishers, 2001.
- [2] R. Hanssen, Atmospheric heterogeneities in ERS tandem SAR interferometry. Delft, DEOS Report No 98.1, 1998.
- [3] T. Oguchi, "Electromagnetic wave propagation and scattering in rain and other hydrometeors," Proc. IEEE, vol. 71, pp. 1029-1077, 1983.
- [4] J. Marshall and W. Palmer, "The distribution of raindrops with size," J. Meteorol., 5, pp. 165-166, 1948.
- [5] H. C. Van de Hulst, Light Scattering by Small Particles, New York, John Wiley, 1957.
- [6] H. Pruppacher and K. Beard, "A wind tunnel investigation of the internal circulation and shape of water drops falling at terminal velocity" in air, Q. J. R. Meteorol. Soc., vol 96, pp. 247-256, 1970
- [7] M. Costantini, "A Novel Phase Unwrapping Method Based on Network Programming," IEEE Trans. Geosci. Remote Sens., vol. 36, No 3, pp. 813-821, 1998.
- [8] J. Saastamoinen, "Introduction to Practical Computation of Astronomical Refraction," Bulletin Geodesique, vol. 106, pp. 383-397, 1972.
- [9] M. Bevis, S. Chiswell, S. Bussinger, T. A. Herring and Y. Bock, "Estimating wet delays using numerical weather analysis and predictions," Radio Science, vol. 31, No 3, pp. 477-487.